

Origins of Mechanical Strength and Elasticity in Thermally Reversible, Acrylic Triblock Copolymer Gels

Peter L. Drzal and Kenneth R. Shull*

Department of Materials Science and Engineering, Northwestern University, Evanston, Illinois 60208-3108

Received August 2, 2002

ABSTRACT: Thermoreversible gels were formed by dissolving a poly(methyl methacrylate)–poly(*tert*-butyl acrylate)–poly(methyl methacrylate) triblock copolymer in a variety of alcohols, including ethanol, 1-butanol, 2-ethylhexanol, and 1-octanol. The gels exhibit an ideal and reversible solid/liquid transition in each of these solvents, behaving as strong elastic solids at room temperature and as freely flowing liquids above the gel transition. The time-dependent elastic properties of the gels are governed by two transition temperatures. The first transition is the critical micelle temperature (cmt) near 60 °C, below which the PMMA blocks aggregate to form a physically cross-linked network. As the gels are cooled to room temperature, differential scanning calorimetry (DSC) reveals a second transition where the PMMA domains undergo a glass transition. The glass transition temperature of the PMMA domains increases when the gels are aged at room temperature. Time–temperature superposition can be applied below the cmt to give master curves describing the relaxation behavior of the gels in the vicinity of the glass transition of the PMMA domains. These relaxation times increase by 1 decade for every 8 K decrease in temperature, a result that is consistent with previous measurements of polymer relaxations in the vicinity of the glass transition temperature.

Introduction

In recent years, physically associating ABA type triblock copolymer gels have attracted considerable scientific and technical interest. These gels are formed when a triblock copolymer is dissolved in a solvent selective for the midblock.^{1–3} In conditions where the solvent is not able to dissolve the endblocks, these blocks aggregate to form spherical domains. If the concentration of triblock copolymer molecules is sufficiently large, a certain fraction of the midblocks will form bridges between the endblock domains, resulting in the formation of an elastic network. The shear modulus of the gel is determined by the molar concentration of bridging molecules, which is in turn given by $f\phi/V_0$, where f is the fraction of bridging molecules, ϕ is the triblock copolymer volume fraction, and V_0 is the copolymer molar volume. An estimate for the shear modulus of the gel is obtained from simple rubber elasticity theory:⁴

$$G = \phi f R T / V_0 \quad (1)$$

where R is the gas constant and T is the absolute temperature.

Physical gels formed from associating triblock copolymers have been made utilizing both aqueous and nonaqueous solvent systems. Aqueous systems have particular technological interest in bioerodible and biocompatible scaffold networks for drug delivery and wound healing.⁵ Scientifically, these systems have been used for a variety of fundamental studies on phase behavior^{6,7} and rheological response.^{2,8–11} Nonaqueous gels have typically been formed with triblock copolymers consisting of relatively short glassy endblocks and a rubbery midblock. Those most commonly studied were formed from commercially available triblock copolymers with poly(styrene) endblocks and either a poly(isoprene)

or a poly(ethylene/butylene) midblock. A significant body of research has been dedicated to understanding the structural morphologies^{12–19} and viscoelastic^{3,20–22} properties of these systems in hydrocarbon oils.

The physical process controlling the relaxation times of these gels involves the exchange of endblocks in and out of the aggregates. Ordered systems consisting of glassy aggregates generally have good creep resistance because of the mechanical strength and long relaxation times associated with the glassy domains. The response of an ideal thermoreversible gel is controlled by the relative location of two transition temperatures. The first of these is the critical micelle temperature (cmt), below which aggregation of the endblocks occurs.²³ This transition is fundamentally the same for both diblocks and triblocks, although the formation of an elastic network at the cmt occurs only for triblock copolymers. The second transition corresponds to the glass transition of the endblock aggregates. Thermoreversible materials generally rely on just one of these transitions. For example, styrenic thermoplastic elastomers consist of aggregated polystyrene endblocks in a low- T_g matrix phase with a composition corresponding to that of the midblock. At room temperature the relaxation times of the glassy domains are very large, and the ordered material is a strong elastic solid with a high creep resistance. When heated above the polystyrene glass transition temperature, the mechanical strength and relaxation times of the polystyrene domains decrease substantially, so that these materials can be melt processed. Further reduction in the viscosity of the system requires that a transition to a fully disordered state also be accessible, i.e., that the cmt (equivalent to the order–disorder temperature for a neat block copolymer) not be too high.

In order for a triblock copolymer solution to exhibit a fast, reversible transition between a low-viscosity liquid state and a high-strength elastic state, the two transi-

* To whom correspondence should be addressed.

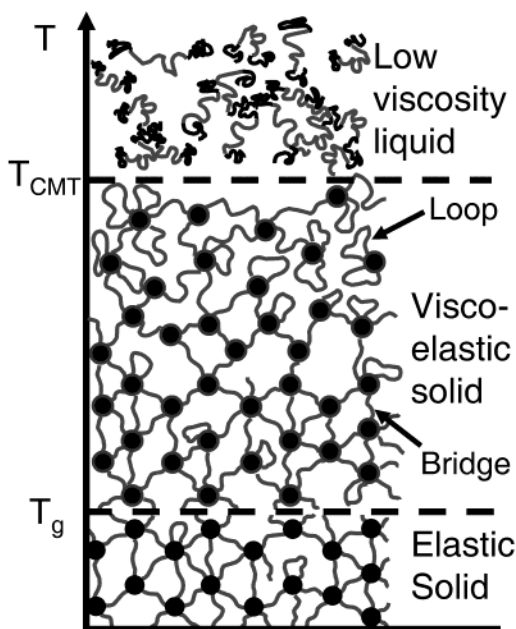


Figure 1. Schematic illustration of the solid/liquid transition of the acrylic triblock copolymers studies in this paper.

tions discussed above must be in relatively close proximity to one another, with the $cmt > T_g$ as illustrated schematically in Figure 1. The ordered elastic state is formed at the critical micelle temperature. Because the ordered domains are not glassy at the cmt , an equilibrated microstructure forms rapidly at this temperature. Further cooling below T_g is required to enhance the creep resistance of this ordered phase. It is rare for a triblock copolymer solution to fulfill all of the criteria necessary for both of these transitions to be located in a useful temperature range. The triblock copolymer should have a midblock that is soluble in the solvent at all temperatures and endblocks that are soluble at high temperatures, but not at low temperatures. In addition, the glass transition temperature of the solvent-swollen endblock domains should be somewhere between the cmt and the use temperature (typically room temperature) of the solid gels.

In this paper we describe a set of acrylic triblock copolymer gels that meet all of these criteria. These gels are based on triblock copolymers consisting of a poly(*tert*-butyl acrylate) (PtBA) midblock and poly(methyl methacrylate) (PMMA) endblocks. Solutions of these block copolymers in a variety of alcohols have a critical micelle temperature near 60 °C and a glass transition temperature for the PMMA domains that varies between 35 and 50 °C. These qualities are unique to this system and are due to the temperature dependence of thermodynamic interactions between the PMMA endblocks and the solvent. Our detailed focus in this paper is largely on the properties of these materials in the ordered state and on the role of the glass transition on the stress relaxation behavior of the gels.

Experimental Section

Materials. Thermoreversible triblock copolymer gels were prepared by dissolving an anionically polymerized PMMA–PtBA–PMMA triblock copolymer in one of several different alcohols that are selective for the midblock. A more detailed description of the triblock copolymer synthesis²⁴ and a structural characterization²⁵ of the triblock copolymer gel have been provided previously. Briefly, a difunctional organolithium

initiator was used to initiate the polymerization of the *tert*-butyl acrylate monomer in tetrahydrofuran, in the presence of an excess of LiCl. Methyl methacrylate monomer was then added to the living polymer solution to complete the triblock copolymer. Using a Waters Breeze GPC and a Waters 410 refractive index detector calibrated with poly(styrene) standards in tetrahydrofuran, the total molecular weight of the triblock copolymer was determined to be 139 000 g/mol (66 wt % PtBA) and to have a polydispersity index of 1.15. Part of the polydispersity is due to the termination of some reactive sites on the difunctional initiator prior to the polymerization step. The resulting polymer is a blend consisting of diblock and triblock chains, with a diblock weight fraction of approximately 0.1. A few experiments were also performed with a similar triblock copolymer with PMMA endblocks and a poly(*n*-butyl acrylate) (PnBA) midblock, kindly provided by Prof. R. Jerome. This copolymer was synthesized by atom transfer radical polymerization²⁶ and has a total molecular weight of 138 000 g/mol (78 wt % PnBA).

Methods. Homogeneous solutions consisting of 15 vol % triblock copolymer were formed in ethanol, 1-butanol, 2-propanol, 2-ethyl-1-hexanol, or 1-octanol and heated to a temperature near 70 °C. Transparent gels formed immediately when the solutions were cooled to room temperature. Rheological characterization was conducted using a Paar Physica MCR-300 rheometer with a double-gap cylinder measuring system (DG26.7). The temperature-dependent dynamic moduli of the gels were measured at 1% applied strain, which was determined to be in the linear regime. Heating and cooling rates of 1.1 °C/min were applied during thermal cycling. Stress relaxation experiments were also performed. In these experiments, a circular column of gel with a diameter of 1 cm and of thickness of 5 mm was placed within a temperature-controlled solvent chamber. A flat, stainless steel punch with a radius (a) of 495 μ m was mounted in series with a force transducer, linear stepping motor, and a displacement sensor. A LabVIEW program collected load and displacement data while simultaneously controlling motor movement. The average stress under the punch is given by $P/\pi a^2$. During stress relaxation experiments, the stepping motor advanced the probe at 25 μ m/s into the column of gel up to a distance δ and maintained that displacement within $\pm 0.500 \mu$ m. Relaxation data from the first 100 s were excluded because of the finite loading rate. The circular columns of gel were made by heating the thermoreversible gel above the gel transition to 75 °C and pouring it into a PDMS mold with a 1 cm diameter. Upon cooling to room temperature, the gels were removed from the mold and either immediately tested or aged in a closed chamber under 2-ethylhexanol vapors.

Differential scanning calorimetry (DSC) scans of the gels were obtained using a TA Instruments 2920 MDSC in standard mode. Hermetically sealed aluminum DSC pans were used for these measurements to avoid solvent evaporation. The instrument was calibrated using standard calibration techniques with indium as the standard. Gel samples were isothermally aged at 23 °C for time periods up to 130 days and were analyzed while heating at 5 °C/min to 90 °C. The samples were then cooled to 25 °C at 5 °C/min.

Results and Discussion

In a previous research report with a similar acrylic triblock copolymer gel, the structural morphology of these gels was examined with small-angle X-ray scattering.²⁵ Gelation in these materials conforms to the endblock aggregation process outlined in the Introduction. Below the gel transition, the poly(methyl methacrylate) endblocks aggregate into nanometer size spherical domains that are randomly distributed and interconnected with the solvated PtBA chains.²⁵ The aggregated PMMA domains form the physical cross-linking sites responsible for the elastic nature of the gel, and the molecular weight between entanglements (i.e., the molecular weight of the midblock) largely deter-

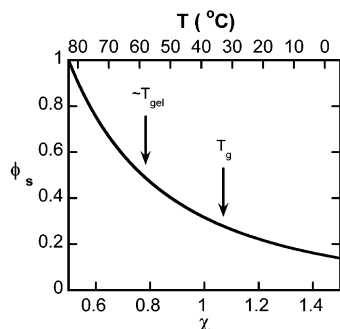


Figure 2. Plot of the volume fraction of solvent for a high molecular weight polymer immersed in pure solvent as a function of the Flory–Huggins interaction parameter. The temperature scale is obtained from the measured temperature dependence of the interactions between PMMA and 1-butanol (eq 3). The gel temperature and PMMA glass transition temperature for the acrylic gels in 1-butanol are also indicated.

mines the elastic modulus of the gel. From eq 1, 3700 Pa is predicted as an upper estimate of the room temperature equilibrium shear modulus assuming a bridging factor of 1, a midblock molecular weight of 100 000 g/mol, and a density of about 1 g/cm³. This value is about a factor of 2 larger than the measured value of 1780 Pa.

Above the gel transition, the endblocks dissociate, producing a freely flowing liquid with the viscosity of a simple polymer solution. The strong temperature dependence of the PMMA/solvent interactions is responsible for the temperature dependence of the transition. As the temperature is further decreased below the gel temperature, the rubbery PMMA domains become glassy and undergo physical aging at room temperature.

The cmt and the value of T_g for the PMMA domains can be understood in terms of the equilibrium swelling of PMMA by the solvent. If a polymer is immersed in a solvent bath, the equilibrium swelling of the polymer is determined by a chemical potential balance between solvent molecules located in the bath and in the polymer. The Flory–Huggins expression for the solvent chemical potential in high molecular weight polymer solution provides a useful way of presenting the results that we have obtained:²⁷

$$\mu_s = \ln \phi_s + (1 - \phi_s) + \chi(1 - \phi_s)^2 \quad (2)$$

where ϕ_s is the solvent volume fraction and χ is the polymer/solvent interaction parameter and μ_s is the solvent chemical potential. If μ_s is known, eq 2 can be used to obtain the relationship between ϕ_s and χ . In our case the solvent bath corresponds to the solvated midblock and can be treated approximately as a pure solvent, with $\mu_s = 0$. The resulting relationship between ϕ_s and χ is shown in Figure 2. Application of this plot to a specific polymer/solvent pair requires that the temperature dependence of χ be known. The temperature scale at the top of Figure 2 is for the PMMA/1-butanol system and was obtained from the following measured temperature dependence of χ obtained from viscometric and sedimentation behavior:^{28,29}

$$\chi = 1.4508 - 0.0115T \quad (3)$$

with T in °C. Included in the figure are the approximate gel temperature and the glass transition for the triblock copolymer in butanol. For $\chi < 0.5$, the solvent is a good

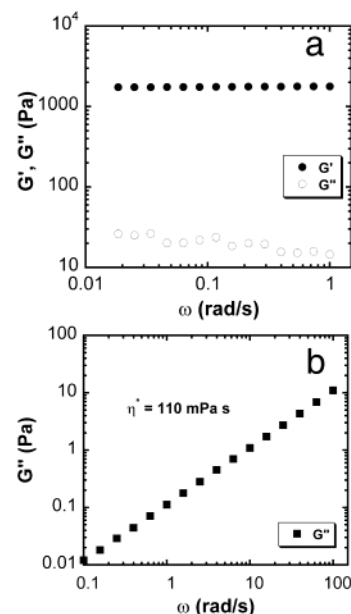


Figure 3. Rheological characterization of the elastic and liquid states for a 2-ethylhexanol triblock copolymer gel with $\phi_p = 0.15$: (a) storage and loss moduli at 25 °C; (b) loss modulus at 75 °C, illustrating a Newtonian response with a viscosity of 110 mPa s.

solvent for the endblocks. Endblock aggregation is not expected under these circumstances. The θ temperature, corresponding to the temperature for which $\chi = 0.5$, is therefore an upper limit for the critical micelle temperature.

The arrows in Figure 2 indicate the measured locations of the cmt and of the PMMA glass transition for 1-butanol solutions of the triblock copolymer. The cmt is less than the θ temperature because the block copolymers are made more soluble by the presence of the midblock chains. Lodge et al.³⁰ have obtained similar results for the aggregation of diblock copolymer molecules in highly selective solvents. As indicated in Figure 2, the expected solvent volume fraction in the PMMA domains at the critical micelle temperature is ~ 0.50 . The PMMA domains are still rubbery under these conditions but expel additional solvent as the system is cooled and χ increases. The exclusion of solvent eventually leads to a glass transition in the PMMA domains, resulting in an enhanced elastic response of the gels at room temperature. In the following subsections we discuss the rheological signature of the gel transition at the critical micelle temperature, the calorimetric signature of the PMMA glass transition, and the effect of this glass transition on the stress relaxation behavior of the gels.

Rheological Characterization of the Gel Transition. The ideal nature of the solid/liquid transition of triblock solutions in 2-ethylhexanol (chosen because of its low vapor pressure) is illustrated by the data in Figures 3 and 4. The frequency dependence of the dynamic moduli in the solid and liquid states is illustrated in Figure 3. The ideal elastic nature of the gels at 25 °C is illustrated by the data in Figure 3a. The measured storage moduli (G') dominate the loss moduli (G'') by 2 orders of magnitude and exhibit little frequency dependence over the range of angular frequencies tested. The elastic properties of these gels when formed with alcohols exhibit little creep behavior and no change in short-term evolution of modulus.²⁴

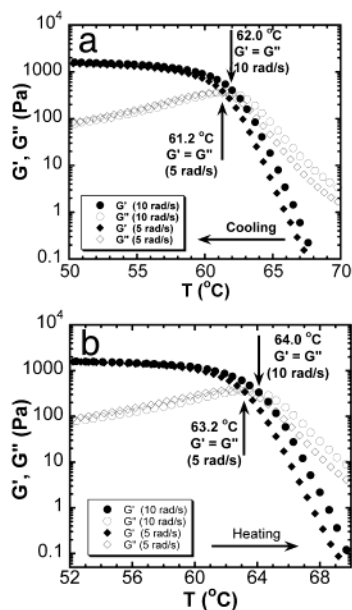


Figure 4. Temperature dependence of the storage and loss moduli for a 2-ethylhexanol triblock copolymer gel with $\phi_p = 0.15$: (a) data obtained during cooling at 1.1 °C/min; (b) data obtained during heating at 1.1 °C/min.

Figure 3b illustrates the liquidlike properties of the triblock solutions when heated to 75 °C, approximately 12 °C above the gel transition. At this temperature the solution behaves as a Newtonian liquid with a viscosity of 110 mPa s, only 10 times the viscosity of pure 2-ethylhexanol at room temperature. This low viscosity at elevated temperatures, along with the elastic properties at room temperature, provides great flexibility in processing applications like thermoreversible gel casting of ceramic materials, where the ideal solid/liquid transition is maintained even when these materials are highly filled with rigid particles.³¹

Figure 4 shows the dynamic moduli measured upon heating and cooling in the vicinity of the gel transition. The rapid change in the shear moduli by 3 orders of magnitude over a five degree region above and below the gel transition is indicative of the structural change in these gels. The approximate liquid to solid transition, referred to as the gel point, can be determined by identifying the temperature where the storage and loss moduli are equal. Dynamic moduli obtained at frequencies of 5 and 10 rad/s show a weak frequency dependence of the gel temperature. The same weak frequency dependence is observed on cooling (Figure 4a) and on heating (Figure 4b). The temperature hysteresis of the gel temperature is relatively small, with the gel temperature on heating being just 2 °C higher than the gel temperature measured on cooling.

Thermal Characterization of the PMMA Glass Transition. Calorimetric traces for a 2-ethylhexanol gel with $\phi_p = 0.15$ are presented in Figure 5. One trace corresponds to a gel that was heated after 130 days of aging at room temperature in a hermetically sealed DSC pan that prevented solvent evaporation. A strong endothermic peak was recorded at 52 °C. This transition is 10 deg lower than the gel point measured in rheological studies and does not correspond to the structural transition in previous X-ray scattering work.²⁵ When cooled through the gel point, no measurable exothermic transition corresponding to aggregation is observed. In addition, heating a cooled gel did not yield a measurable

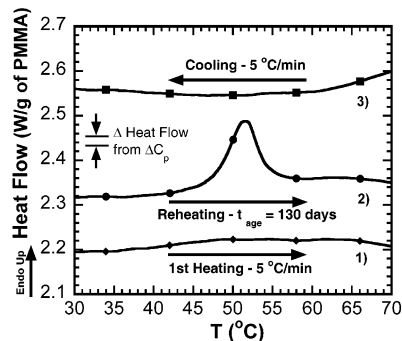


Figure 5. DSC plots of the time-dependent enthalpy of physical aging within the PMMA domains in a 2-ethylhexanol triblock copolymer gel ($\phi_p = 0.15$): (1) unaged gel heated at 5 °C/min; (2) gel aged at room temperature for 130 days and then heated at 5 °C/min; (3) representative curve for aged or unaged gel being cooled at 5 °C/min.

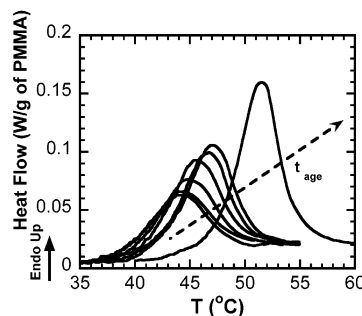


Figure 6. Summary of the endothermic peaks recorded for a 2-ethylhexanol gel with $\phi_p = 0.15$ for aging times up to 130 days. All curves were recorded using a heating rate of 5 °C/min.

enthalpic transition until after at least 2 days of aging at room temperature. The magnitude and peak maximum of the endothermic peak in our gels are time-dependent as summarized in Figure 6, where the endothermic peaks at various aging times are plotted on the same axes. The total integrated enthalpy of the endothermic peak and the temperature corresponding to the peak maximum both increase with aging time. This thermal behavior is characteristic of physical aging.³² It suggests that after aggregation the PMMA domains go through a glass transition. The magnitude of the endothermic peak increases with time because aging reduces the free volume and enthalpy of the PMMA domains.³³ During subsequent heating, equilibration of the enthalpy is measured as an endothermic peak and occurs at the glass transition temperature of the physically aged PMMA. This concept is illustrated schematically in Figure 7. The slopes of the solid lines represent C_{pl} and C_{pg} , the respective heat capacities of the liquid and glassy states of the PMMA domains. On cooling, the glass transition occurs at T_{gc} . At the aging temperature, the enthalpy decreases toward the equilibrium liquid value and is reduced by an amount ΔH_a . During reheating, the enthalpy increases at a rate determined by the heat capacity of the glass. When the temperature reaches the glass transition of the aged PMMA, the material is able to reabsorb the enthalpy required to reach its equilibrium value. The magnitude of this enthalpy gain, referred to as ΔH_r , can be expressed in the following way:

$$\Delta H_r = \Delta H_a + \Delta C_p(T_{gh} - T_{gc}) \quad (4)$$

where $\Delta C_p = C_{pl} - C_{pg}$.

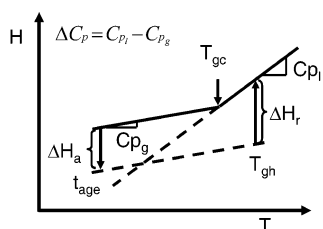


Figure 7. Schematic of the idealized enthalpy vs temperature illustrating the aging effects on the measured enthalpy during differential scanning calorimetry. The respective heat capacities of the liquid and glassy states of the PMMA domains, C_{p_l} and C_{p_g} , are represented by the slopes of the solid lines. T_{gc} is the glass transition obtained on cooling, ΔH_a is the enthalpy decrease during the aging time, and ΔH_r is the enthalpy increase needed to reach equilibrium at T_{gh} , the glass transition obtained during heating of the aged sample.

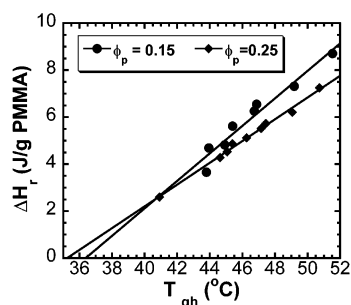


Figure 8. Measured transition enthalpies for 2-ethylhexanol gels with $\phi_p = 0.15$ (circles) and 0.25 (diamonds) as a function of the temperature corresponding to the maximum of the endotherm. Extrapolation of the data to $\Delta H_r = 0$ gives a glass transition for the unaged 2-ethylhexanol gels of ~ 36 °C.

Both glass transition temperatures are expected to be weak functions of the heating and cooling rates that are employed. In addition, T_{gh} depends on the aging time. For zero aging time $\Delta H_a = 0$, and T_{gc} and T_{gh} are expected to be close to one another. Determination of the unaged glass transition can be obtained from the extrapolation of a plot of ΔH_r vs T_{gh} . As illustrated in Figure 8, 2-ethylhexanol gels with triblock volume fractions of 0.15 and 0.25 both give extrapolated glass transitions for the unaged materials of about 36 °C.

The slopes of the curves in Figure 8, and our inability to directly measure the glass transition temperature of an unaged gel, are also consistent with known heat capacity data for PMMA. The slopes of both experimental plots are close to $0.5 \text{ J g}^{-1} \text{ K}^{-1}$, whereas atactic PMMA with a glass transition at 105 °C has $\Delta C_p = 0.34 \text{ J g}^{-1} \text{ K}^{-1}$.³⁴ In fact, ΔC_p is expected to be a lower limit for the slope, because of contributions to the melting endotherm from ΔH_a . As for our inability to directly measure the change in heat capacity directly, this result is also consistent with the expected change in power, obtained by multiplying ΔC_p by our heating rate of 5 K/min. The change in overall heat flow at the PMMA glass transition is approximately 0.028 W/g of PMMA and is included in Figure 5 to illustrate the magnitude of the change in power of a glass transition relative to the heat flow measured during a typical scan. Clearly, a broad glass transition could be indistinguishable within the baseline heat flow, primarily because of the low fraction of PMMA that is present in the gels.

In Figure 9 we show that the physical aging behavior is not exclusive to triblock gels formed in 2-ethylhexanol. Figure 9a shows how the glass transition temperature increases with aging time for each of the alcohols.

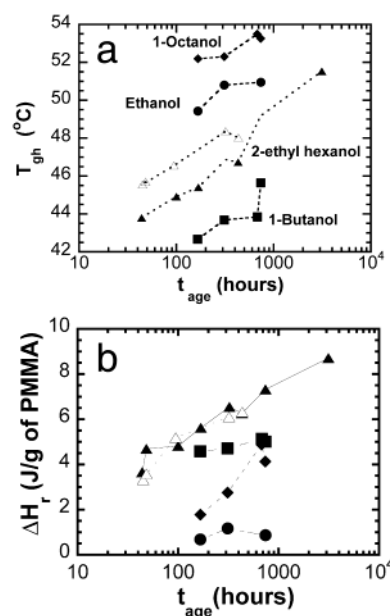


Figure 9. Summary of the thermal properties of aged gels obtained during heating of aged gels at 5 °C/min: (a) peak temperature of the endothermic transition; (b) integrated enthalpy relaxation. Solid symbols correspond to the anionically polymerized PMMA–PtBA–PMMA triblocks dissolved in the alcohols indicated in part a, with $\phi_p = 0.15$. Open triangles correspond to a PMMA–PnBA–PMMA triblock copolymer synthesized by atom transfer radical polymerization, dissolved in 2-ethylhexanol with $\phi_p = 0.10$.

Values of the enthalpy relaxation, normalized by the amount of PMMA in the gels, are plotted vs the aging time in Figure 9b. In addition, we have verified that gelation and physical aging in alcohols are not limited to anionically polymerized triblock copolymers, where the PMMA blocks have a high degree of stereoregularity. This same behavior has been observed in a PMMA–PnBA–PMMA triblock copolymer made from atom transfer radical polymerization. The measured glass transition temperatures and enthalpy relaxations for a 10 vol % ATRP synthesized polymer gel in 2-ethylhexanol have been included in Figure 9. The aging behavior of the ATRP triblock copolymer gel is nearly identical to that of the anionically polymerized triblock copolymer gel. Reported values of the triad composition are 57:37:6 (syndiotactic:heterotactic:isotactic) for PMMA synthesized by ATRP²⁶ and 80:20:0 for PMMA synthesized by ligand anionic polymerization.³⁵ The similarity of behavior for gels formed from triblock copolymers synthesized by these two methods indicates that stereocomplexation within the PMMA domains does not play an important role in either the micellization or the glass transition of these materials in the alcohols that we have used.

The glass transition temperatures measured from the 15 nm PMMA domains in the triblock copolymer gels are consistent with reported values for bulk solvent-swollen PMMA.³⁶ For example, the glass transition temperature for an unaged butanol gel occurs at 32 °C, which according to Figure 2 corresponds to an equilibrium solvent volume fraction of ~ 0.30 . This value is in good agreement with published values of the glass transition of PMMA in butanol.³⁶ Overall, the results of this section demonstrate that the PMMA domains go through a glass transition at a temperature that is above room temperature but below the critical micelle temperature. The strong elastic character of the gels at

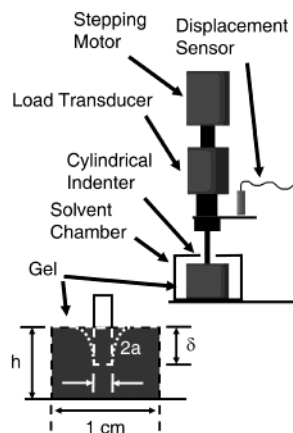


Figure 10. Schematic of the experimental apparatus used for stress relaxation experiments.

room temperature is attributed to this glass transition in the gel, which dramatically lengthens the relaxation times associated with reorganization of the network structure. These longer relaxation times are not readily studied by oscillatory rheometry but are more easily probed by the time-domain experiments described in the following section.

Stress Relaxation Experiments. A schematic illustration of the experimental apparatus used for stress relaxation experiments is shown in Figure 10. The compressive load, P , and displacement, δ , are measured as a flat, cylindrical punch is pressed into a thick sample of gel. In our case the displacement is fixed, and the time-dependent load is used to obtain the relaxation modulus, utilizing the following expression:^{37,38}

$$E(t) = \frac{3P(t)}{8a\delta} \quad (5)$$

where a is the radius of the cylindrical punch. Experiments were conducted in the linear regime, where $E(t)$ is independent of the applied displacement. This linear regime persisted to relatively large displacements, equal to several times the punch radius. In some cases, stress relaxation moduli were well described by the following power law form:

$$E(t) = E_{\text{ref}}(t/t_{\text{ref}})^{-\lambda} \quad (6)$$

where t_{ref} is an arbitrary reference time, which we typically take as 1000 s. The important quantity in the stress relaxation experiments is the value of the power law exponent. The exponent provides a measure of the viscoelasticity of the gel, where larger values correspond to a larger viscoelastic loss. Power law type expressions to fit stress relaxation data from physically associating systems are common.^{39–42}

The relaxation moduli collected at 23 °C for unaged gels and gels aged for 30 days are shown in Figure 11. Each sample was loaded to an average stress of 32 kPa, after which the stress was allowed to relax for 10 000 s at a fixed strain. The measured power law decreased from 0.032 ± 0.001 to 0.016 ± 0.003 due to aging effects. Aging in the PMMA domains reduces the free volume and increases the glass transition relative to the testing temperature. Consequently, the required force to pull a PMMA chain from the spherical domain increases. Increased stress levels of 45 and 65 kPa were also tested

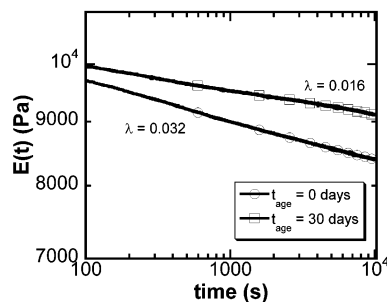


Figure 11. Stress relaxation moduli over 1000 s obtained for an unaged gel (circles) and a gel aged for 30 days (squares).

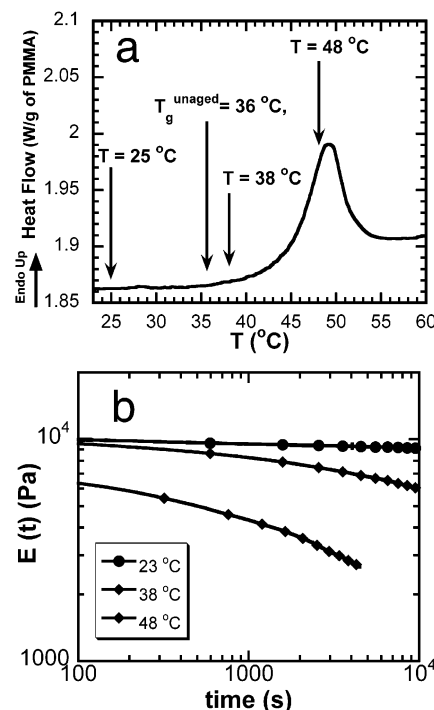


Figure 12. Stress relaxation experiments for a 2-ethylhexanol gel with $\phi_p = 0.15$ that had been aged for 30 days at room temperature: (a) thermogram of the aged gel during heating, illustrating the three different temperatures at which the stress relaxation experiments were conducted; (b) relaxation moduli obtained at these three different temperatures.

to probe the stress required to activate increased viscoelastic loss in the form of chain pullout at room temperature. Up to the applied stress of 65 kPa little change is measured on the relaxation behavior of the gels.

Stress relaxation experiments at various temperatures were conducted to probe the kinetic state of the PMMA domains via the relaxation behavior of the gels. To eliminate effects associated with aging of the gels that occurs during the relaxation test, gels that had been previously aged for 30 days were used in these experiments. The locations of the testing temperatures relative to the measured glass transition of the aged gel are included in Figure 12a. The relaxation data at these temperatures are summarized in Figure 12b. At temperatures below the glass transition of the PMMA domains, the relaxation behavior obeys the power law type behavior described above. When the temperature is increased above the onset of the glass transition, enhanced stress relaxation is observed, and a power-law stress relaxation function no longer describes the

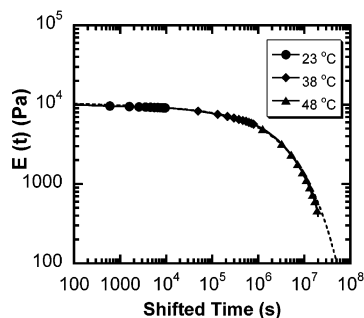


Figure 13. Master curve obtained from time–temperature superposition for a series of stress relaxation experiments at various temperatures. Gel samples were aged for 30 days. A reference temperature of 23 °C is used for shifting. The dashed line represents eq 8, with $\tau = 3 \times 10^6$ s.

data. A stretched exponential of the following form is ample in capturing this relaxation behavior:

$$E(t) = E_{\text{ref}} \exp[-(t/\tau)^\beta] \quad (7)$$

Use of a stretched exponential is common for similar systems above or near the glass transition.³⁹

The effect of an increase in temperature is to decrease the relaxation time of the gel network. Time–temperature superposition can be used to collapse data taken at a variety of temperatures onto a single master curve. The results of this superposition are illustrated in Figure 13, where relaxation curves are plotted as a function of the shifted time t/a_t for the aged gels. The shift factor a_t is equal to 1 at 23 °C, 1.2×10^{-2} at 38 °C, and 5.0×10^{-4} at 48 °C. Combining the power law type behavior (eq 6) to describe relaxation below the glass transition and stretched exponential behavior (eq 7) to describe relaxation near or above the glass transition, the following equation can be used to describe the entire master curve:

$$E(t) = 10000(t/1000)^{-0.016} \exp[-(t/\tau)^{0.5}] \quad (8)$$

This expression is included in Figure 13 with $\beta = 0.53$ and $\tau = 3.06 \times 10^6$ s. This very large relaxation time corresponds to the reference temperature of 23 °C, which is approximately 25 deg below the glass transition of the aged PMMA domains.

Comparison to Other Systems. The relaxation time obtained from Figure 13 agrees well with the relaxation time reported by Hotta et al.³⁹ for a nonreversible triblock copolymer with spherical glassy end-blocks of comparable molecular weight at an analogous distance below T_g . This similarity is illustrated in Figure 14, where we plot the relaxation times from our thermoreversible system and those from Hotta et al. as a function of the proximity to the glass transition. The relaxation times from Hotta et al. are from their fits of stress relaxation data using a stretched exponential similar to eq 7 but with $\beta = 0.2$. Relaxation times at each measured temperature were determined by applying the appropriate shift factors found in their paper. The glassy nature of the aggregates is responsible for the long relaxation times at room temperature. The temperature dependence in both cases (1 decade change in relaxation time for a temperature change of 8–12 °C) is also similar to the temperature dependence of relaxations in the vicinity of the glass transition, further confirming that our fundamental interpretation of the

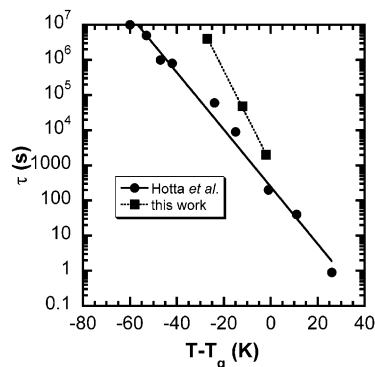


Figure 14. Comparison of the relaxation times of the thermoreversible gels and a nonreversible triblock copolymer (Hotta et al.³⁹) with similar spherical glassy domains.

relaxation processes in terms of an underlying glass transition is sensible.⁴³ Systems with nonglassy aggregates, such as hydrophobically modified water-soluble polymers used as associative thickeners, have much shorter relaxation times and also undergo shear thinning at relatively low stress levels.^{2,6}

Relaxation times similar to those obtained for systems with glassy aggregates can be found in reversible gels formed by the crystallization of the physical cross-linking sites.^{44–46} Stress relaxation experiments on these systems give power law stress relaxation exponents between 0.01 and 0.03. Gels with crystallizing aggregates can be highly elastic, but long times are generally required for gelation. Gelatin, for example, is commonly used throughout the food industry because of its ability to form strong gels. A 1.95 wt % solution of gelatin requires approximately 1 h to gel at 23 °C.⁴⁷ After gelation, the modulus continues to evolve over time and can require between 100 and 150 h to reach its plateau. These complex aging effects are representative of the behavior of gels that form as a result of some type of crystalline order.

The rapid, reversible gelation of our acrylic triblock copolymer gels, with an elastic modulus that is independent of the aging time, is a unique feature of this system that can be attributed to the ordering and glass transition processes illustrated schematically in Figure 1. Because these processes depend on the nature of the thermodynamic interactions between the solvent and the PMMA blocks of the copolymer, different solvent systems will often give very different results. For example, the gelation process of similar triblock copolymers in *o*-xylene is fundamentally different.^{48,49} While a clear gel transition is observed in this solvent, the low-temperature gel phase exhibits substantial creep behavior, with a short-term elastic modulus that continues to evolve when the samples age at temperatures below the gel point. Association of the PMMA in these cases is attributed to the intramolecular coil-to-helix transition followed by the association of these helices creating the physical network.^{50–53} The role of solvent in these systems has been shown to contribute to the stability of the PMMA helix through solvent–polymer complexes.^{54,55} Moduli obtained with these associating gels at similar volume fractions of polymer are much lower than the moduli obtained in our system. Unlike these and many other physically associating gels, the concentration of load-bearing network strands in our system is determined by the fixed structure of the gel, giving a predictable and reproducible elastic response that does

not evolve during the aging process.

Conclusions

Rheometry, thermal analysis, and mechanical testing have been used to examine the origins of elasticity in physically associating all-acrylic ABA triblock copolymer gels, formed in a variety of alcohols. Alcohols, which are selective solvents for the *tert*-butyl acrylate midblock, create polymer gels with two governing transition temperatures: the critical micellization temperature near 60 °C and the glass transition temperature of the aggregated PMMA endblocks. We measure the unique properties of this system in the context of the temperature-dependent thermodynamic interactions between the PMMA and solvent. Our main conclusions are as follows:

1. Above the cmt, the gel becomes a freely flowing Newtonian liquid, with a viscosity of 110 mPa s at 75 °C.

2. Cooling through the cmt results in the rapid aggregation of PMMA chains due to the strong temperature dependence of the PMMA/alcohol interaction parameter.

3. Thermal analysis reveals the existence of the glass transition temperature of the PMMA domains and the physical aging of these domains at room temperature.

4. At room temperature, which is below the glass transition of the PMMA domains, the gels exhibit ideally elastic behavior with little creep behavior and an elastic modulus that is independent of the aging time.

5. Stress relaxation experiments measure the increase in the relaxation time of the network due to the physical aging effects. Aging contributes to the enhanced creep resistance of the gels by increasing the glass transition temperature but does not affect the rapid and reversible solid/liquid transition.

6. Tacticity of the PMMA domains does not play an important role in the ordering or glass transition processes, and thermoreversible gels with similar properties can be made from triblock copolymers synthesized by anionic polymerization or atom transfer radical polymerization.

Acknowledgment. This work was supported by the National Science Foundation, through the MRSEC program at the Materials Research Center of Northwestern University (DMR-0076097), and through an individual investigator grant (DMR-9975468). The authors also acknowledge Prof. Samuel I. Stupp for the generous use of the TA Instruments 2920 MDSC, Prof. John M. Torkelson use of the Waters GPC, and Prof. Wesley Burghardt for use of the Paar Physica rheometer. We are grateful to Ms. Maisha Gray and Mr. Andy Lebovitz for assistance with the GPC. Finally, we acknowledge Prof. R. Jerome for supplying the ATRP triblock copolymer sample.

References and Notes

- Hamley, I. W. *The Physics of Block Copolymers*; Oxford University Press: Oxford, 1998.
- Annable, T.; Buscall, R.; Ettelaie, R.; Whittlestone, D. *J. Rheol.* **1993**, *37*, 695.
- Watanabe, H.; Kuwahara, S.; Kotaka, T. *J. Rheol.* **1984**, *28*, 393.
- Gent, A. N. In *Engineering with Rubber*; Gent, A. N., Ed.; Hanser Publishers: Munich, 2001; p 37.
- Peppas, N. A. In *Biomaterials Science: An Introduction to Materials in Medicine*; Ratner, B. D., Hoffman, A. S., Schoen, F. J., Lemons, J. E., Eds.; Academic Press: San Diego, 1996; p 60.
- Tae, G.; Kornfield, J. A.; Hubbell, J. A.; Johannsmann, D.; Hogen-Esch, T. E. *Macromolecules* **2001**, *34*, 6409.
- Li, H.; Yu, G. E.; Price, C.; Booth, C.; Hecht, E.; Hoffmann, H. *Macromolecules* **1997**, *30*, 1347.
- Clement, F.; Johner, A.; Joanny, J. F.; Semenov, A. N. *Macromolecules* **2000**, *33*, 6148.
- Serero, Y.; Jacobsen, V.; Berret, J. F.; May, R. *Macromolecules* **2000**, *33*, 1841.
- Serero, Y.; Aznar, R.; Porte, G.; Berret, J. F.; Calvet, D.; Collet, A.; Viguier, M. *Phys. Rev. Lett.* **1998**, *81*, 5584.
- Berret, J. F.; Serero, Y.; Winkelman, B.; Calvet, D.; Collet, A.; Viguier, M. *J. Rheol.* **2001**, *45*, 477.
- Soenen, H.; Liskova, A.; Reynders, K.; Berghmans, H.; Winter, H. H.; Overbergh, N. *Polymer* **1997**, *38*, 5661.
- Kleppinger, R.; Reynders, K.; Mischenko, N.; Overbergh, N.; Koch, M. H. J.; Mortensen, K.; Reynaers, H. *Macromolecules* **1997**, *30*, 7008.
- Kleppinger, R.; van Es, M.; Mischenko, N.; Koch, M. H. J.; Reynaers, H. *Macromolecules* **1998**, *31*, 5805.
- Kleppinger, R.; Mischenko, N.; Reynaers, H. L.; Koch, M. H. J. *J. Polym. Sci., Part B: Polym. Phys.* **1999**, *37*, 1833.
- Kleppinger, R.; Mischenko, N.; Theunissen, E.; Reynaers, H. L.; Koch, M. H. J.; Almdal, K.; Mortensen, K. *Macromolecules* **1997**, *30*, 7012.
- Mischenko, N.; Reynders, K.; Koch, M. H. J.; Mortensen, K.; Pedersen, J. S.; Fontaine, F.; Graulus, R.; Reynaers, H. *Macromolecules* **1995**, *28*, 2054.
- Mortensen, K.; Almdal, K.; Kleppinger, R.; Mischenko, N.; Reynaers, H. *Physica B* **1997**, *241*, 1025.
- Laurer, J. H.; Khan, S. A.; Spontak, R. J.; Satkowski, M. M.; Grothaus, J. T.; Smith, S. D.; Lin, J. S. *Langmuir* **1999**, *15*, 7947.
- Soenen, H.; Berghmans, H.; Winter, H. H.; Overbergh, N. *Polymer* **1997**, *38*, 5653.
- Quintana, J. R.; Diaz, E.; Katime, I. *Macromolecules* **1997**, *30*, 3507.
- Laurer, J. H.; Mulling, J. F.; Khan, S. A.; Spontak, R. J.; Bukovnik, R. *J. Polym. Sci., Part B: Polym. Phys.* **1998**, *36*, 2379.
- Hanley, K. J.; Lodge, T. P.; Huang, C. I. *Macromolecules* **2000**, *33*, 5918.
- Mowery, C. L.; Crosby, A. J.; Ahn, D.; Shull, K. R. *Langmuir* **1997**, *13*, 6101.
- Flanigan, C. M.; Crosby, A. J.; Shull, K. R. *Macromolecules* **1999**, *32*, 7251.
- Tong, J. D.; Moineau, G.; Leclerc, P.; Bredas, J. L.; Lazzaroni, R.; Jerome, R. *Macromolecules* **2000**, *33*, 470.
- Flory, P. *Principles of Polymer Chemistry*; Cornell University Press: Ithaca, NY, 1953.
- Jenckel, V. E.; Gorke, K. Z. *Naturforsch.* **1950**, *5A*, 556.
- Llopis, J.; Albert, A.; Usobiaga, P. *Eur. Polym. J.* **1967**, *3*, 259.
- Lodge, T. P.; Pudil, B.; Hanley, K. J. *Macromolecules* **2002**, *35*, 4707.
- Montgomery, J. K.; Drzal, P. L.; Shull, K. R.; Faber, K. T. *J. Am. Ceram. Soc.* **2002**, *85*, 1164.
- Petrie, S. E. B. *J. Polym. Sci., Part A2: Polym. Phys.* **1972**, *10*, 1255.
- Struik, L. C. E. *Physical Aging in Amorphous Polymers and Other Materials*; Elsevier: Amsterdam, 1978.
- Gaur, U.; Lau, S. F.; Wunderlich, B. B.; Wunderlich, B. *J. Phys. Chem. Ref. Data* **1982**, *11*, 1065.
- Wang, J. S.; Jerome, R.; Warin, R.; Teyssie, P. *Macromolecules* **1993**, *26*, 5984.
- Andrews, E. H.; Levy, G. M.; Willis, J. J. *Mater. Sci.* **1973**, *8*, 1000.
- Johnson, K. L. *Contact Mechanics*; Cambridge University Press: Cambridge, 1985.
- Shull, K. R. *Mater. Sci. Eng. Rep.* **2002**, *36*, 1.
- Hotta, A.; Clarke, S. M.; Terentjev, E. M. *Macromolecules* **2002**, *35*, 271.
- Fazel, Z.; Fazel, N.; Guenet, J. M. *J. Phys. II* **1992**, *2*, 1745.
- Dardin, A.; Spiess, H. W.; Stadler, R.; Samulski, E. T. *Polym. Gels Network* **1997**, *5*, 37.
- Quintana, J. R.; Hernaez, E.; Katime, I. *J. Phys. Chem. B* **2001**, *105*, 2966.
- Ediger, M. D.; Angell, C. A.; Nagel, S. R. *J. Phys. Chem.* **1996**, *100*, 13200.
- Mutin, P. H.; Guenet, J. M. *Macromolecules* **1989**, *22*, 843.

- (45) Lin, Y. G.; Mallin, D. T.; Chien, J. C. W.; Winter, H. H. *Macromolecules* **1991**, *24*, 850.
- (46) He, X. W.; Herz, J.; Guenet, J. M. *Macromolecules* **1987**, *20*, 2003.
- (47) te Nijenhuis, K. In *Thermoreversible Networks. Viscoelastic Properties and Structure of Gels*; Springer: Berlin, 1997; p 160.
- (48) Yu, J. M.; Jerome, R.; Teyssie, P. *Polymer* **1997**, *38*, 347.
- (49) Yu, J. M.; Dubois, P.; Teyssie, P.; Jerome, R.; Blacher, S.; Brouers, F.; Lhomme, G. *Macromolecules* **1996**, *29*, 5384.
- (50) Berghams, H.; Donkers, A.; Frenay, L.; Stoks, W.; Deschryver, F. E.; Moldenaers, P.; Mewis, J. *Polymer* **1987**, *28*, 97.
- (51) Berghmans, M.; Thijs, S.; Cornette, M.; Berghmans, H.; Deschryver, F. C.; Moldenaers, P.; Mewis, J. *Macromolecules* **1994**, *27*, 7669.
- (52) Buyse, K.; Berghmans, H.; Bosco, M.; Paoletti, S. *Macromolecules* **1998**, *31*, 9224.
- (53) Spevacek, J.; Schneider, B. *Adv. Colloid Interface Sci.* **1987**, *27*, 81.
- (54) Spevacek, J.; Suchoparek, M. *Macromolecules* **1997**, *30*, 2178.
- (55) Saiani, A.; Spevacek, J.; Guenet, J. M. *Macromolecules* **1998**, *31*, 703.

MA021255V